



# Scoping Study of Effects on the Advanced Test Reactors Center Flux Trap Due to Various Loadings in the H and Inner A Test Positions

August 2022

*Changing the World's Energy Future*

Tristen Jeda Rogers



#### **DISCLAIMER**

This information was prepared as an account of work sponsored by an agency of the U.S. Government. Neither the U.S. Government nor any agency thereof, nor any of their employees, makes any warranty, expressed or implied, or assumes any legal liability or responsibility for the accuracy, completeness, or usefulness, of any information, apparatus, product, or process disclosed, or represents that its use would not infringe privately owned rights. References herein to any specific commercial product, process, or service by trade name, trade mark, manufacturer, or otherwise, does not necessarily constitute or imply its endorsement, recommendation, or favoring by the U.S. Government or any agency thereof. The views and opinions of authors expressed herein do not necessarily state or reflect those of the U.S. Government or any agency thereof.

# **Scoping Study of Effects on the Advanced Test Reactors Center Flux Trap Due to Various Loadings in the H and Inner A Test Positions**

**Tristen Jeda Rogers**

**August 2022**

**Idaho National Laboratory  
Idaho Falls, Idaho 83415**

**<http://www.inl.gov>**

**Prepared for the  
U.S. Department of Energy  
Under DOE Idaho Operations Office  
Contract DE-AC07-05ID14517**

**Scoping Study of Effects on the Advanced Test Reactor's Center Flux Trap  
Due to Various Loadings in the H and Inner A Test Positions**

Contributing Authors: Tristen J. Rogers (SULI Intern)

INL: Idaho National Lab

ISU: Idaho State University

## **Abstract**

**This study determined the effects experienced by the In-Pile Tube, of the Advanced Test Reactor's center flux trap, due to various loading configurations of the H and Inner A positions. The effects of concern included: the axial profile of the linear heat generation rate of each fuel rodlet, the axial flux shape, and spectrum, in the fuel, and cladding, of each rodlet, and the total fission heating rate of the entire In-Pile Tube. Additionally, the reactivity worth of each configuration, relative to an ATR configuration with water filling all concerning test positions, was determined. The test positions were filled with commonly used test specimens, backup test specimens, and homogeneous substances. The study was performed using the modeling software MCNP6.2.**

## Table of Contents

Section	Page Number
1. Introduction .....	3
2. Theory .....	4
3. Equipment and Procedure .....	7
4. Results .....	10
5. Conclusion .....	16
6. Acknowledgments .....	17

## List of Figures

Figure	Page Number
Figure 1.1: H and Inner A Test Positions .....	4
Figure 2.1: ATR Cross-Section Diagram .....	6
Figure 3.1: IPT Center Rodlet Clusters .....	7
Figure 3.2: IPT Radial Orientation .....	8
Figure 4.1: Averaged Flux Values for BOC_1, Tier 1 .....	13
Figure 4.2: Averaged LHGR for BOC_1, Tier 1 .....	13
Figure 4.3: BOC_15, Tier 1 Thermal Flux Spectrum .....	14
Figure 4.4: BOC_15, Tier 1 Epithermal Flux Spectrum .....	15
Figure 4.5: BOC_15, Tier 1 Fast Flux Spectrum .....	16
Figure 4.4: BOC_15, Tier 1 LHGR Spectrum .....	17

## List of Tables

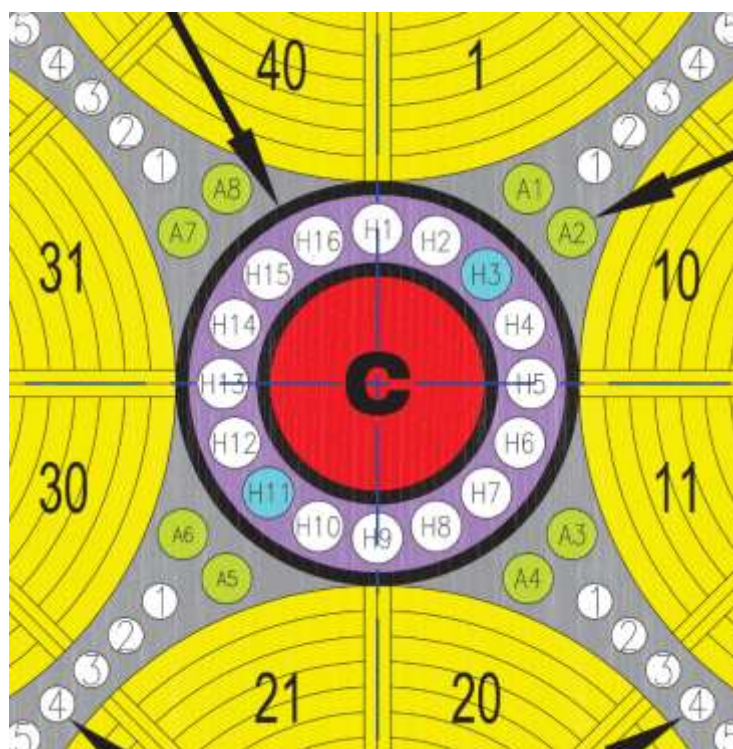
Table	Page Number
Table 3.1: Neutron Energy Ranges .....	10
Table 4.1: Symmetric Loading Configurations .....	11
Table 4.2: Asymmetric Loading Configurations .....	11

## Introduction

This study is focused on analyzing the heat generated by a test sample of nuclear fuel, placed in the Advanced Test Reactor's (ATR) Center Flux Trap (CFT), and the quantity of neutrons (neutron density/flux), of varying kinetic energy, that the fuel is subjected to. This study is concerned with how these quantities will change depending on the loading configuration, of the test specimen positions, immediately surrounding the CFT. These being the H and Inner A positions. This information is vital to the designing of tests, and prolonged studies, to be performed in the ATR. If a fuel sample gets too hot, it could cause mechanical failures to occur to itself or the reactor components surrounding it. For example, if the fuel gets hot enough, it could thermally expand enough to come in contact with, and apply undue mechanical stress to, the fuel cladding. If the fuel gets hotter still, it could melt and release fission products into the reactor core. Additionally, knowing the neutron flux is vital since all reaction rates, in the nuclear fuel, are direct products of the neutron density present in the fuel. This includes the fuel's heating rate. Additionally, if a test specifies the amount of neutron fluence that a fuel specimen is to be subjected to, knowing the neutron flux, experienced by the test specimen, determines how long the specimen is to be irradiated for.

This study is performed using version 6.2 of a simulation software, called MCNP, that can model the behavior of neutrons in a reactor system. The fueled test specimens, used in this study, were designed to be representative of various types of fuel specimens that could, theoretically, be loaded into the CFT, of the ATR. The contents, filling the H and Inner A test positions, consist of typical, non-fueled, test specimens. A diagram of these test positions is shown in Figure 1.1. For academic studies, various, non-standard, backup test specimens were also used to fill the concerning H and A test positions.

**Figure 1.1: H and Inner A Test Positions**



## Theory

Nuclear power, for commercial electricity production, is produced by maintaining a nuclear fission chain reaction. Generally, the chain reaction starts when a neutron, with a thermal energy level (kinetic energy  $\approx 0.025$  electron-volt), is absorbed into a heavy isotope. This heavy isotope is, typically, Uranium-235, which is combined with other elements to form the fuel of a reactor. In the ATR, to distinguish it from test specimens, the nuclear fuel that sustains the chain reaction, is referred to as the “driver” fuel. Upon neutron absorption, the uranium atom will then split apart into two lighter atoms, and emit, on average, 2.43 neutrons. This reaction is known as nuclear fission. Through various interactions/collisions, between the products of this reaction, and the surrounding medium, approximately 200 million electron-volts (MeV), of energy, are produced. On a macroscopic scale, this energy takes the form of heat. As such, the heat



generated in the fuel test specimens, analyzed in this model, is produced by uranium fission. The neutrons generated, from this fission, serve the purpose of eventually being absorbed in other uranium 235 atoms, and causing further fissions. However, when a fission neutron is first produced, it will possess a kinetic energy too high to induce fission. This is known as a fast neutron. Thus, it is slowed down to a thermal energy level by colliding with atoms of a similar atomic mass.

The population of free neutrons is described using a value known as the neutron flux. The neutron flux, or just “flux”, is defined as the number of neutrons, per unit area, per unit time. While free neutrons can be generated in many ways, the fission chain reaction is largely driven by fission neutrons. Because neutrons initiate uranium fission, the amount of heat produced, in the fuel of every reactor, is directly proportional to the value of the neutron flux in that fuel. The value for the neutron flux will not be uniform throughout the entire reactor, and will, generally, be higher, closer towards its center.

MCNP6.2 is a simulation software, described, in its user’s manual, as a “general-purpose, continuous-energy, generalized-geometry, time-dependent Monte Carlo code designed to track many particle types over broad ranges of energies.” Monte Carlo codes use computational algorithms, to solve complicated equations, using repeated random sampling. Using these techniques, MCNP6.2 can simulate the life of a free neutron while traveling through one, or many, mediums. This program, amongst many other things, can simulate the behavior of a nuclear reactor under various operating conditions. This is done by building a geometric model, of the reactor, and specifying the nature, and number, of neutrons whose “life” you want simulated within the model. A large quantity of simulated neutrons, in a reactor model, is representative of the flux, that would be present, in a real version of the reactor. MCNP6.2 is

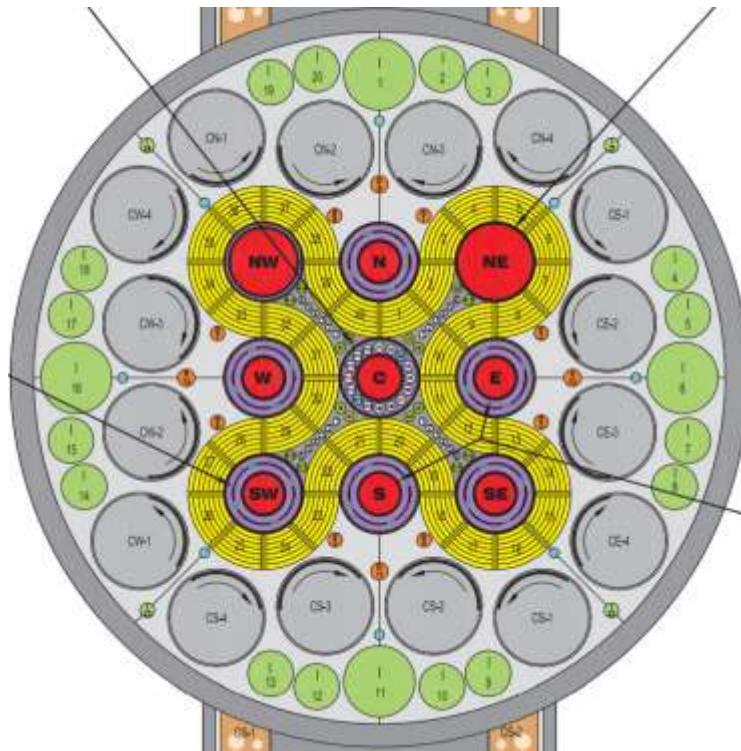
used by, first, writing an input file. This file defines: the surfaces of each component in the reactor, the components themselves, and all the materials used in the reactor design. The individual components, or cells, as they are known in the program, are designed by defining a material that is bounded by a collection of surfaces. The MCNP6.2 input file should also specify the number neutron generations, and numbers of neutrons per generation, to be simulated.

Relevant output data is provided in a text file. Different output information is requested, in the input file, using tallies. Tallies specify what information is wanted in the MCNP output file, and what surfaces, or cells, the information is meant to pertain to.

The ATR is cooled using water that is pressurized at 2.5MPa. Its operating temperature is anywhere between 125°F and 160°F. Since it is a test reactor, it produces no electricity, but rather, is designed to produce a far higher neutron flux than that of reactors found in commercial power plants. Because of this, one of ATR's uses is to test, over a short period of time, how a reactor component will behave, over a long period of time, in a commercial reactor. The reactor contains 77 test specimen positions. The serpentine driver fuel arrangement, of the ATR, is designed to "wrap" around, and form areas of high neutron flux in, nine of these test positions. As such, these nine test positions are known as flux traps. Being pertinent to this study, the ATR produces an average thermal flux value of  $4.4\text{E}+14 \frac{\text{neutrons}}{\text{cm}^2*\text{sec}}$ , and an average fast flux of  $9.7\text{E}+13 \frac{\text{neutrons}}{\text{cm}^2*\text{sec}}$ , in the CFT, with the reactor operating at 110 MW ("Nuclear Material").

Figure 2.1 is an enlarged image of the ATR's core, with the previously described features being visible. Each flux trap is labeled with their cardinal directions, relative to the CFT (labeled "C" in figure). Due to the cloverleaf shape of the fuel, the neutron flux, and subsequent power output, of the four corner lobes, and the CFT, can differ greatly from each other.

**Figure 2.1: ATR Core Cross-Section**



## **Equipment and Procedures**

The purpose of this study is to analyze how the flux, and the heating rate, of a representative fuel test specimen, placed in the CFT, will change depending on the test specimen content, of the H and Inner A test positions. The fuel test specimen contains 6 clusters of six fuel rodlets, evenly stacked above one another. Each rodlet contains ten, stacked, cylindrical fuel pellets that will be, approximately, 0.82 cm wide and 1.05 cm tall. These pellets will be surrounded by helium gas. The helium and pellets are encased in a 0.9778 cm wide, 15.19 cm tall, enclosed zircalloy tube. All the rodlet clusters are housed within a 114.747 cm tall, 4.354 cm wide, circular zircalloy tube. Above, and below, this larger tube, are stainless steel spacers. These spacers keep the Zircalloy tube centered, such that the radial centerlines of the zircalloy tube, and the entire reactor core, are at the same elevation. This entire assembly is known as the

In-Pile Tube (IPT). Figure 2.1 shows a plotted depiction of the two center sections of rodlet clusters, hereafter known as tiers, housed in the modeled IPT. Figure 2.2 is a horizontal cross section showing the IPT's orientation, about its long axis, within the reactor model.

**Figure 3.1: IPT Center Rodlet Clusters**

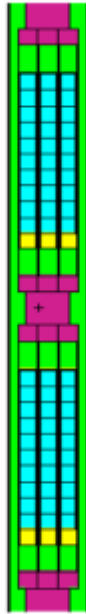


**Figure 3.2: IPT Radial Orientation**



The candidate test specimens, meant to fill the H and Inner A test positions, consist of the following: a high specific activity (HSA) Cobalt target, a low specific activity (LSA) Cobalt target, a General Electric, Boron Carbide, control rod, a Neptunium target, meant to produce plutonium when irradiated, and a solid flow restrictor outboard position (SFROP) filler.

Secondary candidates include Hafnium, Cadmium, dense Boron, and Beryllium fillers.

The data, for this study, is generated by running several MCNP6.2 simulations, with each simulated model having a different test specimen configuration, in the H and Inner A positions.

To streamline the process of building multiple input files, each specimen model is built in their own “universe”, which is a collection of cells that can be repeated. The universes, containing test specimens, are called to the main model, replicated, and moved to their correct locations, and orientations. In this study, the process described, in the previous sentence, is accomplished with a single line of text.

The model, used in this study, is modified from the BuildATR model. It has been rewritten so that every test specimen, in its own respective universe, is placed in every test position. This is done using the single line of text mentioned at the end of the previous paragraph. Specifying which test specimen goes in each position, is done by commenting out all these lines of text, except the line concerning the test specimen you want in that position. Using this technique, the configuration of the concerning test positions is changed by editing, only, a few characters of text, in the input file.

F4, and F7, tallies are, respectively, used to obtain the neutron flux, and the fission energy deposition, average over a specified cell. The Linear Heat Generation Rate (LHGR), of each fuel pellet, is calculated using Equations 3.1, and 3.2. It is done by, first, calculating the Neutron Heat Generation Rate (NHGR). (GDE-594) In Equation 3.1, the F7 tally for each fuel

pellet is given as F7: n.  $n_f$  represents the unit of neutrons generated from fission, and g is a unit of grams. The middle value, in Equation 3.1, is the prompt heating normalization factor (PHNF).

**Equation 3.1**

$$NHGR = \left( F7: n \frac{MeV}{g * n_f} \right) * \left( 1.215 * 10^4 \frac{n_f * W}{MeV * MW} \right) * (Core Power in MW)$$

**Equation 3.2**

$$LHGR = \frac{(NHGR) * (Pellet Mass)}{(Pellet Height)}$$

The total neutron flux, in each fuel pellet, is calculated using Equation 3.3, with the F4 tally given as F4: n. (ECAR-4474) The middle value, of this equation, is the neutron flux conversion factor (NFCF).

**Equation 3.3**

$$\Phi_n = \left( F4: n \frac{n}{cm^2 * n_f} \right) * \left( 7.583 * 10^{16} \frac{n_f}{MW * sec} \right) * (core power in MW)$$

Because free neutrons can exist with a range of kinetic energies, an F4 tally is given for each, of three, energy ranges, for each fuel pellet. These ranges are specified in Table 3.1.

**Table 3.1: Neutron Energy Ranges**

Range Title	Min. Kinetic Energy (MeV)	Max. Kinetic Energy (MeV)
Thermal	0	0.625E-6
Epithermal	0.625E-6	1
Fast	1	20

The results, of every simulated model, will be presented in the form of two graphs for each tier of rodlets. The first will contain three plots showing the thermal, epithermal, and fast flux profiles averaged over every rodlet in the tier. The second will be the LHGR profile, also averaged over every rodlet in the tier. Three additional graphs are given for any model possessing an asymmetric loading configuration, in the H and Inner A positions, about the north-

south axis of the core. An asymmetric loading may cause the flux between the “west” and “east” side of the flux trap to be notably different. This is because a non-fueled test specimen will absorb some of the neutron population surrounding it, with its level of absorption dependent on its composition. Each graph will pertain to a different neutron energy range and will contain plots describing the flux profiles of each rodlet separately. Subsequently, the graphs for each tier can be compared between other tiers in the same, and different models for future ATR experiment designs.

## Results

Initially, nineteen different configurations were modeled. The configurations of the symmetric loadings are shown in Table 4.1, with the asymmetric loadings shown in Table 4.2.

**Table 4.1: Symmetric Loading Configurations**

<b>Input File Titles</b>	<b>Inner A Positions</b>	<b>H Positions</b>
<b>BOC_LSA_HSA</b>	LSA Cobalt Target	HSA Cobalt Target
<b>BOC_LSA_LSA</b>	LSA Cobalt Target	LSA Cobalt Target
<b>BOC_HSA_LSA</b>	HSA Cobalt Target	LSA Cobalt Target
<b>BOC_Co</b>	HSA Cobalt Target	Odd Number = HSA Co Even Number = LSA Co
<b>BOC_PFS_HSA</b>	PFS Neptunium Target	HSA Cobalt Target
<b>BOC_PFS_PFS</b>	PFS Neptunium Target	PFS Neptunium Target
<b>BOC_HSA_PFS</b>	HSA Cobalt Target	PFS Neptunium Target
<b>BOC_HSA_B<sub>4</sub>C</b>	HSA Cobalt Target	B <sub>4</sub> C Control Rod
<b>BOC_PFS_B<sub>4</sub>C</b>	PFS Neptunium Target	B <sub>4</sub> C Control Rod
<b>BOC_B<sub>4</sub>C_PFS</b>	B <sub>4</sub> C Control Rod	PFS Neptunium Target
<b>BOC_PFS_Be</b>	PFS Neptunium Target	Beryllium Filler
<b>BOC_PFS_Hf</b>	PFS Neptunium Target	Hafnium Filler
<b>BOC_PFS_B</b>	PFS Neptunium Target	Dense Boron Filler
<b>BOC_PFS_Cd</b>	PFS Neptunium Target	Cadmium 113 Filler
<b>BOC_PFS_H<sub>2</sub>O</b>	PFS Neptunium Target	Water ( $\rho = 0.726$ g/cc)
<b>BOC_PFS_SFROP</b>	PFS Neptunium Target	SFROP

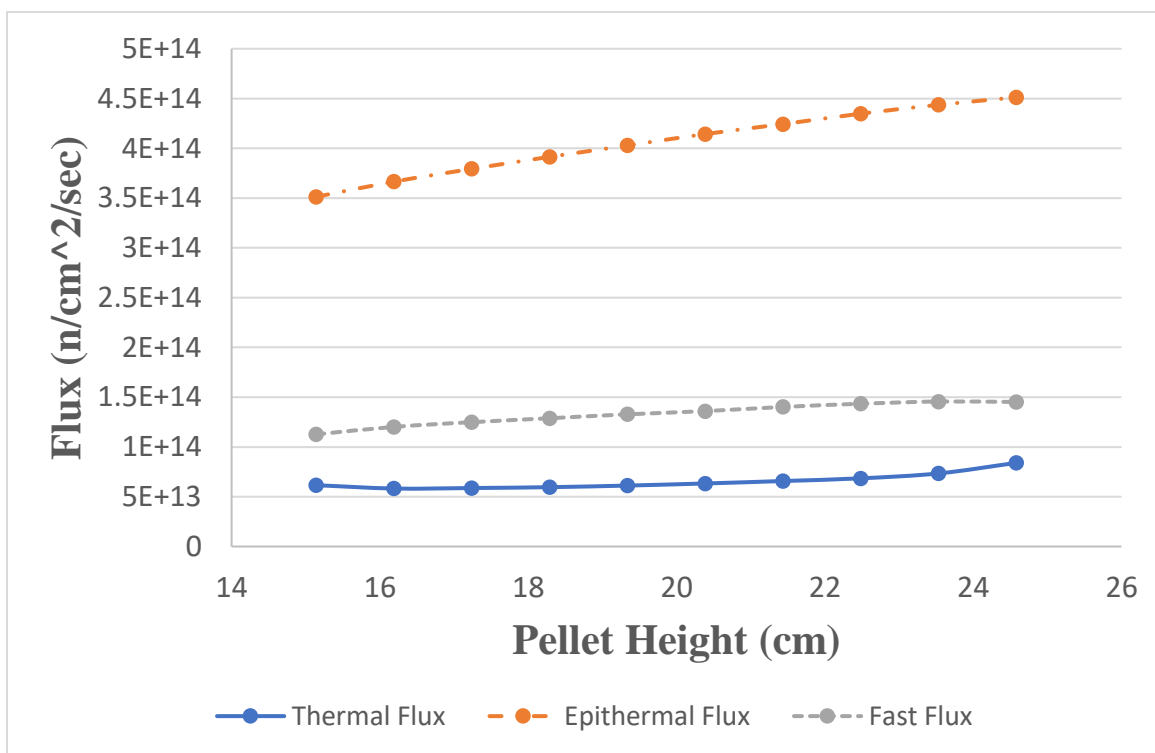
**Table 4.2: Asymmetric Loading Configurations**

<b>Input File Title</b>	<b>A1 – A4</b>	<b>A5 – A8</b>	<b>H1 – H9</b>	<b>H10 – H16</b>
<b>BOC_As_Co</b>	HSA Cobalt	LSA Cobalt	HSA Cobalt	LSA Cobalt
<b>BOC_As_PFS_B<sub>4</sub>C</b>	PFS Np Target	B <sub>4</sub> C Control Rod	PFS Np Target	B <sub>4</sub> C Control Rod
<b>BOC_As_B_SFROP</b>	PFS Np Target	PFS Np Target	Dense Boron	Al Filler

The models, and method for changing the test position configurations, described in the second paragraph of page nine, were successfully built. Error was accounted for by simulating the life of six billion neutrons, per simulation. Simulating this many neutrons ensured that data, for every tally result, possessed a standard deviation between 1% and 0.1%. of the mean value. The uncertainty, associated with the accuracy of the geometry of the model, to that of the real reactor, is beyond the scope of this study. Rather than comparative results, between the In-Pile Tubes of every simulated model, samples of the gathered data are provided in this report.

The presented data pertains to the first tiers of BOC\_LSA\_HSA, and BOC\_AS\_PFS\_B<sub>4</sub>C, and is representative of all the results that will be obtained from each tier, of every model. Figure 4.1 shows the averaged thermal, epithermal, and fast flux values for tier 1 of model BOC\_LSA\_HSA, while Figure 4.2 shows the LHGR for the same tier. Figures 4.3, 4.4, and 4.5 show the thermal, epithermal, and fast flux spectrums, respectively, for each rodlet, in tier one, of the BOC\_AS\_PFS\_B<sub>4</sub>C model. It is observed that the absolute value of the slope, of all the fitted lines, between the first and second pellet, as well as the ninth and tenth pellet, is greater than that of the slope between pellets two and nine. This is likely because pellets two through nine are axially “shielded”, via their adjacent pellets. This prevents them from absorbing as many thermal neutrons, from the surrounding medium, but increases the number of fast neutrons that they absorb from adjacent fuel pellets.



**Figure 4.1: Averaged Flux Values for BOC\_LSA\_HSA, Tier 1****Figure 4.2: Averaged LHGR for BOC\_LSA\_HSA, Tier 1**

**Figure 4.3: BOC As PFS  $B_4C$ , Tier 1 Thermal Flux Axial Profile**

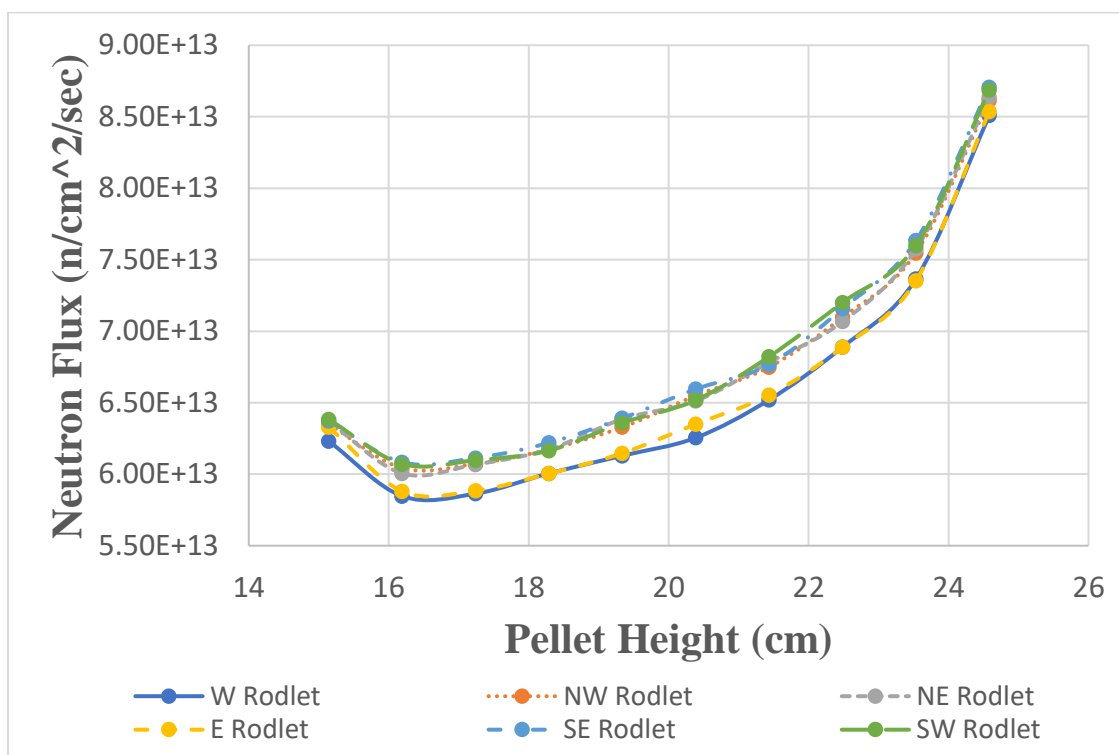


**Figure 4.4: BOC As PFS  $B_4C$ , Tier 1 Epithermal Flux Axial Profile**

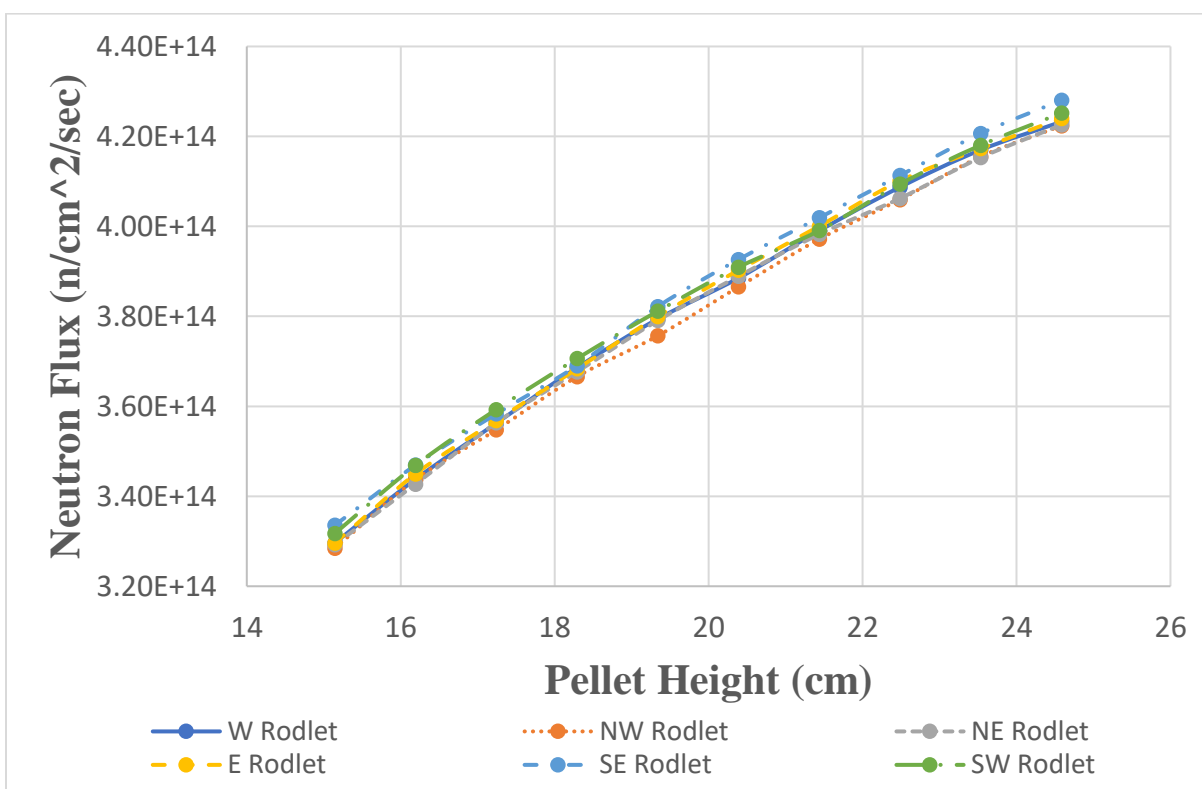


**Figure 4.5: BOC As PFS  $B_4C$ , Tier 1 Fast Flux Axial Profile**

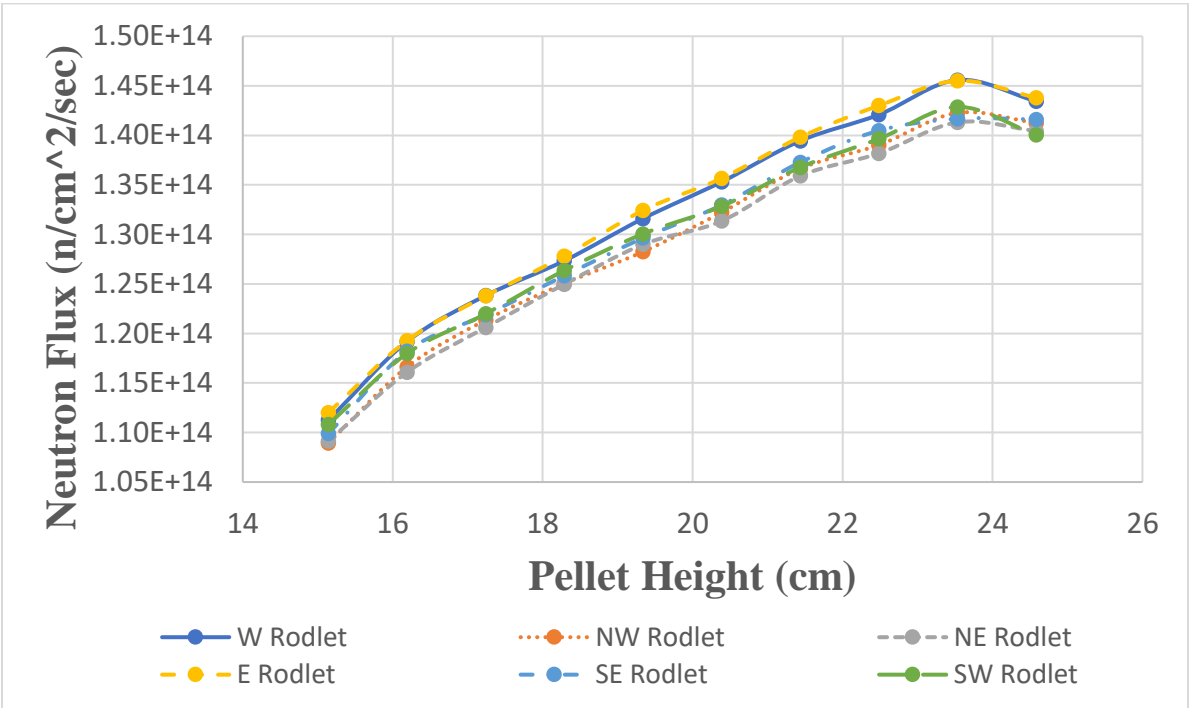
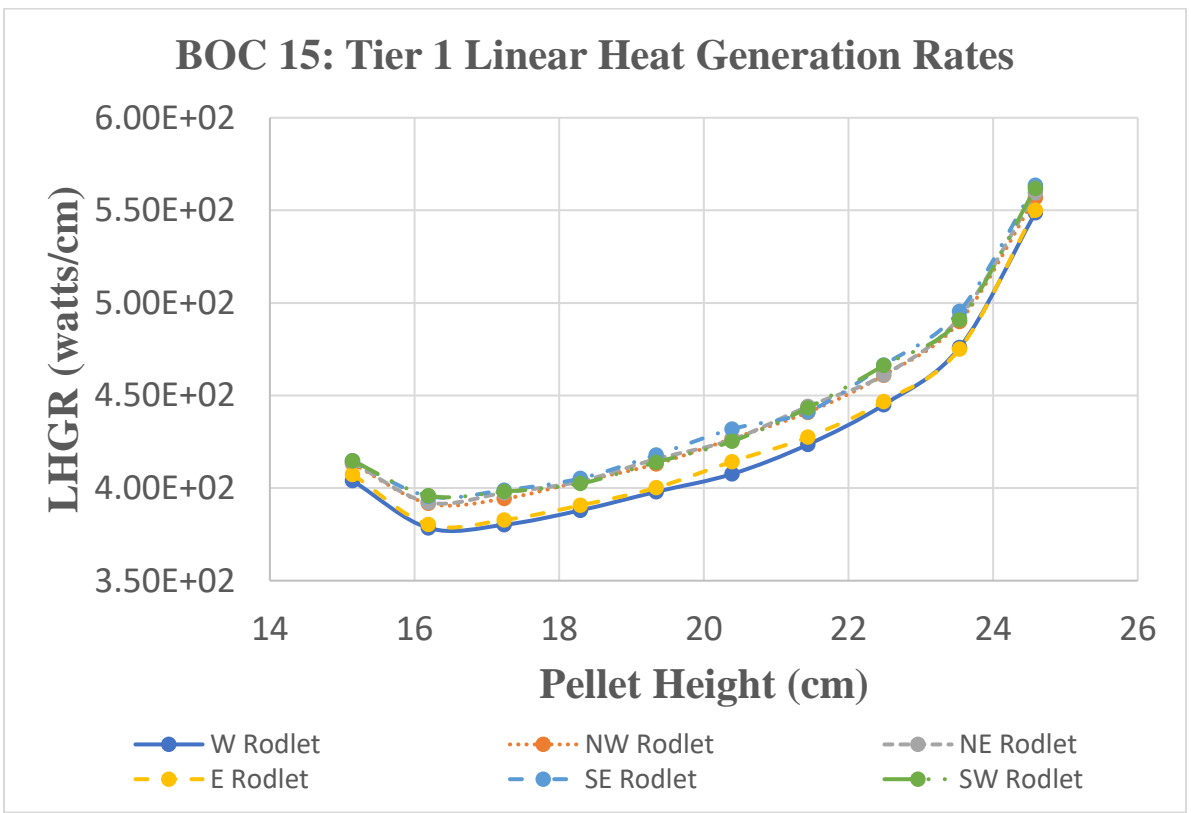


**Figure 4.4: BOC As PFS  $B_4C$ , Tier 1 LHGR Axial Profile**



It should be noted that the thermal flux, and LHGR profiles, for the west and east pins, of BOC\_As\_PFS\_ $B_4C$ , are noticeably less than that of the other pins in their respective graphs. The opposite is true for the fast flux profiles of the same model.

## **Conclusion**

All the various model configurations were simulated without any errors, or significant impediments, and the simulated flux values, for the CFT, are in accordance with empirical data. Each tier, and rodlet's, LHGR and thermal flux spectrum, are reflective of each other. This supports the fact that thermal neutrons induce fission, which leads to heat generation in nuclear fuel. All various flux, and LHGR, profiles will be subject to comparison when designing future test specimen configurations for the ATR. The complete results of this study will be submitted for publication in 2023.

## **Acknowledgements**

I would like to express my sincere gratitude to several people who had a hand in the success of this project.

First, my INL mentor, Travis J. Labossiere-Hickman. His advice, and guidance, was impeccable and vital to the success of the project, and to my understanding of the concepts necessary to complete it. Additionally, he was patient regarding my shortcomings and supportive of my efforts.

Secondly, my on-site mentor, Austin L. Carter. He was always available to help me solve the, in hindsight, quick and simple problems I was dealing with. He also took the time to explain new concepts to me that I had little prior experience in.

Third, Mehmet Turkman, a fellow member of neutronics analysis team, at INL, who explained to me how to set up tallies in a MCNP model that was far more complex than I have ever worked with before.

## References

- ECAR-4474, “ATF-2B Physics Safety Analysis” Rev. 0, September 25, 2019
- February 2016 “ABWR Design Control Document Tier 2” *nrc.gov*, GE Hitachi Nuclear Energy, <https://www.nrc.gov/docs/ML1608/ML16081A093.pdf>.  
July 5, 2022
- GDE-594, “Experiment Design and Analysis Guide – Neutronics and Physics”  
Rev. 2, January 11, 2017
- “Nuclear Material Experiments Irradiated in the Advanced Test Reactor.”  
*nst.inl.gov*.  
<https://nst.inl.gov/irradiationtesting/SitePages/Experiment%20Positions%20in%20Advanced%20Test%20Reactor.aspx>
- Sep. 2011, “Fuel and Control Rods System” General Electric Systems Technology Manual, pg. 2.2-11 to 2.2-12,  
<https://www.nrc.gov/docs/ML1125/ML11258A302.pdf>